


Article

# Crystal Structure and Thermal Behavior of $\text{SbC}_2\text{O}_4\text{OH}$ and $\text{SbC}_2\text{O}_4\text{OD}$

Holger Kohlmann <sup>1,\*</sup> , Anne Rauchmaul <sup>1</sup>, Simon Keilholz <sup>1,2</sup> and Alexandra Franz <sup>3</sup>

<sup>1</sup> Institute of Inorganic Chemistry, Leipzig University, Johannisallee 29, 04103 Leipzig, Germany; a.rauchi@web.de (A.R.); simon.keilholz@uni-leipzig.de (S.K.)

<sup>2</sup> CM CHEMIEMETALL GmbH, Niels-Bohr-Str. 5, 06749 Bitterfeld, Germany

<sup>3</sup> Helmholtz-Zentrum Berlin, Hahn-Meitner-Platz 1, 14109 Berlin, Germany; alexandra.franz@helmholtz-berlin.de

\* Correspondence: holger.kohlmann@uni-leipzig.de; Tel.: +49-341-9736201

Received: 23 December 2019; Accepted: 15 March 2020; Published: 19 March 2020



**Abstract:** The order of OH groups in the crystal structure of  $\text{SbC}_2\text{O}_4\text{OH}$ , a potential precursor in the synthesis of ternary oxides, was debated. Neutron diffraction on the deuteride  $\text{SbC}_2\text{O}_4\text{OD}$  revealed disordered OD groups with half occupation for deuterium atoms on either side of a mirror plane ( $\text{SbC}_2\text{O}_4\text{OD}$  at  $T = 298(1)$  K:  $Pnma$ ,  $a = 582.07(3)$  pm,  $b = 1128.73(5)$  pm,  $c = 631.26(4)$  pm). O–H stretching frequencies are shifted by a factor of 1.35 from  $3390\text{ cm}^{-1}$  in the hydride to  $2513\text{ cm}^{-1}$  in the deuteride as seen in infrared spectra.  $\text{SbC}_2\text{O}_4\text{OH}$  suffers radiation damage in a synchrotron beam, which leaves a dark amorphous residue. Thermal decomposition at 564 K yields antimony oxide, carbon dioxide, carbon oxide, and water in an endothermic reaction. When using  $\text{SbC}_2\text{O}_4\text{OH}$  as a precursor in reactions, however, ternary oxides are only formed at much higher temperatures.

**Keywords:** antimony; oxalate; hydroxide; neutron diffraction; thermal analysis; precursor; radiation damage; isotope effect; deuteration

## 1. Introduction

Metal oxalate hydroxides are a rather rare class of compounds. Some examples are  $\text{Cd}_2\text{C}_2\text{O}_4(\text{OH})_2$  [1],  $\text{ZrC}_2\text{O}_4(\text{OH})_2$  [2],  $\text{BiC}_2\text{O}_4\text{OH}$  [3] and the title compound. Due to their moderate thermal stability, they have been used as precursors in materials synthesis, for instance for the fabrication of metal/metal oxide composites [4]. Antimony oxalate hydroxide,  $\text{SbC}_2\text{O}_4\text{OH}$ , was reported to form by refluxing freshly prepared antimony(III) oxide in oxalic acid and was found as a colorless precipitate when oxalic acid was added to a solution of  $\text{SbCl}_3$  in hydrochloric acid [5]. Its composition was established by chemical analysis, solid-state NMR, infrared spectroscopy, and  $^{121}\text{Sb}$ -Mössbauer spectroscopy [6]. It decomposes within one step at 563 K to antimony(III) oxide [7,8].  $\text{SbC}_2\text{O}_4\text{OH}$  can be used for the preparation of antimony containing compounds, i.e., mixed crystal oxides such as  $\text{BaBi}_{1/2}\text{Sb}_{1/2}\text{O}_3$  [9]. The low decomposition temperature, simple synthesis and stable composition seem to be attractive properties for usage as a precursor for antimony-based materials.

The crystal structure of  $\text{SbC}_2\text{O}_4\text{OH}$  was determined by X-ray powder diffraction to be isotopic to that of  $\text{BiC}_2\text{O}_4\text{OH}$  [3]. Pentagonal  $\text{SbO}_6$  pyramids form zigzag chains linked by OH groups. Each oxalate anion coordinates two antimony cations, thus connecting the chains to build up a three-dimensional framework. Antimony ions are very close to the pentagonal base plane of the pyramids, leaving one side of the cation uncoordinated, which is not uncommon for  $ns^2$  cations such as  $\text{Sb}^{3+}$ . However, the question of hydrogen atom location remains unclear. In  $\text{BiC}_2\text{O}_4\text{OH}$ , hydrogen positions could not be located [3]. In  $\text{SbC}_2\text{O}_4\text{OH}$ , hydrogen atoms were placed on either side of a mirror plane ( $Pnma$ ) with half occupancy. Hints for an ordering of hydrogen atoms in a lower symmetry ( $Pna2_1$ )

were found by quantum-mechanical studies, but not from diffraction experiments [10]. Since hydrogen has a very low atomic form factor as compared to antimony, its contribution to X-ray diffraction patterns is very small, thus probably preventing a clear distinction between ordered and disordered crystal structure. In order to tackle the problem of hydrogen order in antimony oxalate hydroxide, we have synthesized  $\text{SbC}_2\text{O}_4\text{OH}$  and  $\text{SbC}_2\text{O}_4\text{OD}$ , characterized them by a variety of methods, and located hydrogen (deuterium) atoms by neutron diffraction data.

## 2. Results

### 2.1. Infrared Spectra

$\text{SbC}_2\text{O}_4\text{OH}$  shows an O–H stretching frequency of  $3390\text{ cm}^{-1}$  in accordance with earlier results [6]. In the deuterated compound  $\text{SbC}_2\text{O}_4\text{OD}$ , this is shifted to  $2513\text{ cm}^{-1}$ , i.e., by a factor of 1.35 with respect to  $\nu(\text{O–H})$ , while other signals are hardly affected. This isotope effect is close to the theoretically expected value of  $\sqrt{2}$  and in very good agreement with isotope shifts found in other inorganic hydroxides, e.g., 1.36 for  $\text{Mg}(\text{OH})_2$  and  $\text{Mg}(\text{OD})_2$  [11]. Infrared spectra thus prove the deuteration procedure to be successful, but also reveal some remaining hydrogen due to a small remaining signal at  $3390\text{ cm}^{-1}$ . An estimation of integrated peak intensities leads to a deuteration degree of about 80%. This value may be regarded as a rough estimate only, because the base line of infrared spectra is ill defined (Figure 1).

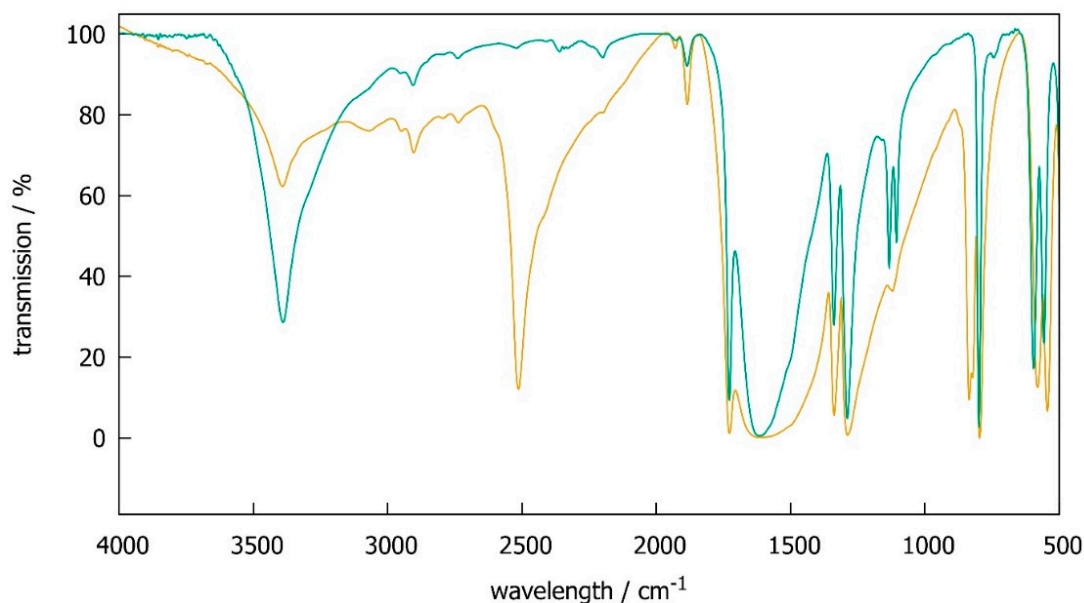


Figure 1. Infrared spectra of  $\text{SbC}_2\text{O}_4\text{H}$  (green) and  $\text{SbC}_2\text{O}_4\text{OD}$  (brown).

### 2.2. X-Ray Powder Diffraction and Rietveld Analysis

X-ray powder diffraction and subsequent Rietveld analysis confirmed the crystal structure model for  $\text{SbC}_2\text{O}_4\text{OH}$  published before [10] and proved the single-phase character of the samples. The patterns showed a strong preferred orientation of crystallites in all samples along [010]. X-ray powder diffraction further proved the deuterated compound  $\text{SbC}_2\text{O}_4\text{OD}$  to be isotopic. Expectedly, X-ray data did not allow for a distinction between the hydrogen-disordered ( $Pnma$ ) and the hydrogen-ordered model ( $Pna2_1$ ), neither for  $\text{SbC}_2\text{O}_4\text{OH}$  nor for  $\text{SbC}_2\text{O}_4\text{OD}$ .

### 2.3. Neutron Powder Diffraction and Rietveld Analysis

Neutron powder diffraction was performed on a deuterated sample in order to avoid the huge incoherent scattering of  $^1\text{H}$  [12]. Rietveld refinements were carried out using the disordered model in

*Pnma* [10] as well as deuterium-ordered crystal structure models. Lowering the symmetry to *Pna2<sub>1</sub>* allows complete ordering of hydrogen (deuterium) atoms. However, refinement with such completely ordered models did not yield better agreement between measured and calculated neutron powder diffraction patterns, as indicated by residual values and graphical representation. A refinement of occupation numbers for both possible deuterium positions with the constraint  $\text{occ}(D1) + \text{occ}(D2) = 1$  yielded  $\text{occ}(D1) = 0.67(5)$  and  $\text{occ}(D2) = 0.33(5)$ , i.e., the difference between both, is only 3.4 combined standard uncertainties and thus, hardly significant. The 1:2 ratio in occupation numbers suggested a tripling of the unit cell, which would allow a sequence + + – (or up, up, down) for the orientation of –OD groups. Refinement attempts with such models did not yield better agreement between measured and calculated neutron powder diffraction patterns either. Another possible ordering is achieved for a deuterium position on a mirror plane, i.e., with  $y = 1/4$  instead of  $\approx 0.28$  (Table 1), however, agreement factors are worse compared to the disordered model and thermal displacement parameters of the deuterium atoms are very large ( $>8 \times 10^4 \text{ pm}^2$ ). Therefore, the crystal structure of  $\text{SbC}_2\text{O}_4\text{OD}$  is described in the disordered *Pnma* model (half occupation by D/H on Wyckoff position  $8d$ ), which gives a very good agreement between measured and calculated neutron powder diffraction patterns (Figure 2, Table 1). As already determined from infrared spectroscopy (Section 2.1), deuteration did not reach completeness. A refinement of H/D occupation yielded 6.4(5)% H and 93.6(5)% D with the constraint  $\text{occ}(H) + \text{occ}(D) = 1/2$ , thus giving the composition  $\text{SbC}_2\text{O}_4\text{D}_{0.936(5)}\text{H}_{0.064(5)}$  for the sample used in neutron diffraction (Table 1). For reasons of simplicity, this is referred to as  $\text{SbC}_2\text{O}_4\text{D}$  in the following. Further details of the crystal structure investigations may be obtained from FIZ Karlsruhe, 76344 Eggenstein-Leopoldshafen, Germany (fax: (+49)7247-808-666; e-mail: crysdata@fiz-karlsruhe.de), on quoting the deposition number CSD-1969091.

**Table 1.** Refined crystal structure of  $\text{SbC}_2\text{O}_4\text{OD}$  at  $T = 298(1) \text{ K}$  and residual values of the Rietveld refinement based on neutron powder diffraction; space group *Pnma*,  $a = 582.07(3) \text{ pm}$ ,  $b = 1128.73(5) \text{ pm}$ ,  $c = 631.26(4) \text{ pm}$ ;  $R_p = 3.0\%$ ,  $R_{wp} = 3.8\%$ ,  $R_{Bragg} = 6.2\%$ ,  $\chi^2 = 1.2$ .

| Atom | Wyckoff Position | <i>x</i>     | <i>y</i>     | <i>z</i>     | $B_{\text{iso}}/10^4 \text{ pm}^2$ | Occupation   |
|------|------------------|--------------|--------------|--------------|------------------------------------|--------------|
| Sb   | 4c               | 0.1799(9)    | 1/4          | 0.5064(8)    | 1.00(12)                           | 1            |
| C    | 8d               | 0.1066(6)    | 0.5245(3)    | 0.5531(5)    | 1.06(7)                            | 1            |
| O1   | 4c               | 0.5373(10)   | 1/4          | 0.7105(10)   | 0.99(13)                           | 1            |
| O2   | 8d               | 0.2600(7)    | 0.4519(4)    | 0.6067(6)    | 1.73(9)                            | 1            |
| O3   | 8d               | 0.1203(7)    | 0.6353(3)    | 0.5827(6)    | 1.23(8)                            | 1            |
| D    | 8d               | 0.6431(16)   | 0.2844(8)    | 0.6076(13)   | 3.81(31)                           | 0.468(5)     |
| H    | 8d               | <i>x</i> (D) | <i>y</i> (D) | <i>z</i> (D) | $B_{\text{iso}}(\text{D})$         | 1/2 – occ(D) |

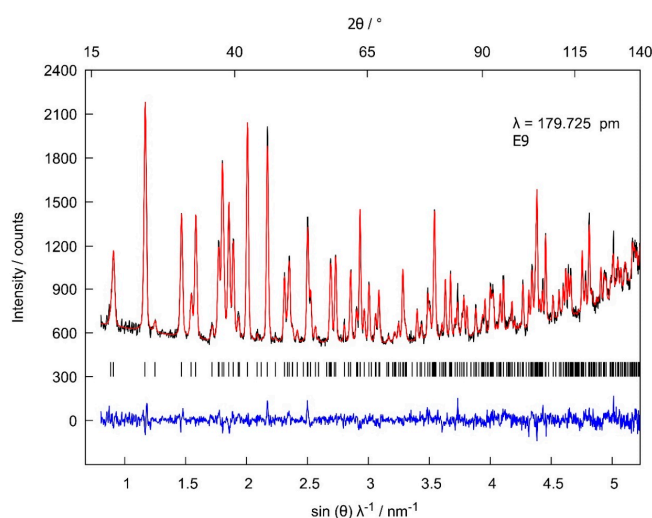


**Figure 2.** Rietveld refinement of the crystal structure of  $\text{SbC}_2\text{O}_4\text{OD}$  at  $T = 298(1) \text{ K}$  based on neutron powder diffraction data (black: measured diffraction data, red: calculated diffraction pattern, blue: difference between measured and calculated pattern, black bars: Bragg reflection markers;  $\lambda = 179.725 \text{ pm}$ ).

#### 2.4. Thermal Analysis: DSC-TG-MS

Thermal analysis for  $\text{SbC}_2\text{O}_4\text{OH}$  shows a single-step decomposition to  $\text{Sb}_2\text{O}_3$  at 564 K (onset temperature of mass loss) in an endothermic reaction (Figure 3). The mass loss of 34.8% agrees well with a calculated value of 35.7% for the reaction  $2 \text{SbC}_2\text{O}_4\text{OH} = \text{Sb}_2\text{O}_3 + \text{H}_2\text{O} + 2 \text{CO}_2 + 2 \text{CO}$ . Evolved gas analysis (EGA) by mass spectrometry (MS) confirms this hypothesis.

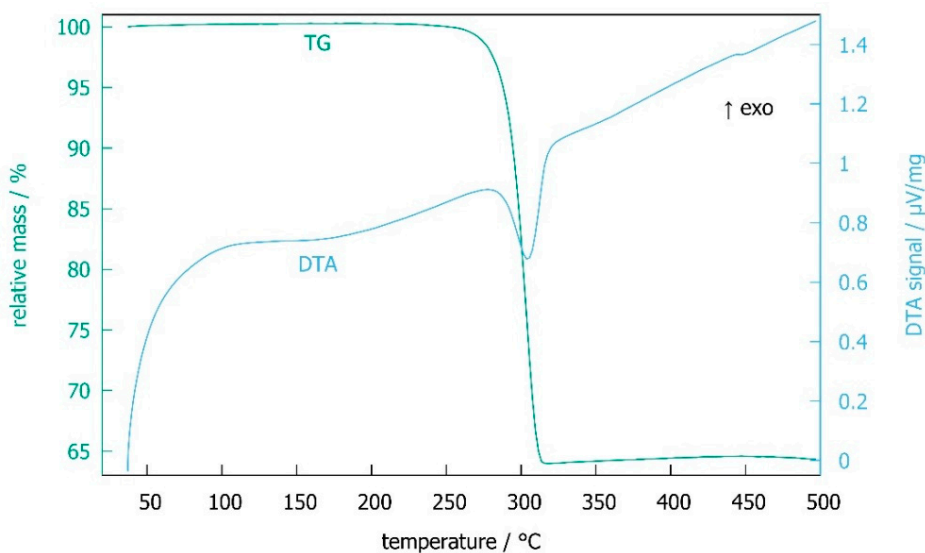


**Figure 3.** Differential scanning calorimetry (blue) and thermogravimetry (green) of  $\text{SbC}_2\text{O}_4\text{OH}$ .

#### 2.5. Radiation Damage

In an attempt to collect high-resolution diffraction data, synchrotron experiments were performed at the beamline PDIFF of ANKA (Ångströmquelle Karlsruhe) of the Karlsruhe Institute of Technology (KIT) at a wavelength of  $\lambda = 112.684(1)$  pm. The sample was contained in a thin-walled glass capillary with a 0.3 mm outer diameter. The diffraction experiment failed, because after exposure to the synchrotron beam for about 1 h, the intensity of Bragg reflections vanished almost completely, indicating that less crystalline material was in the synchrotron beam. Capillary and beam alignment were confirmed to be in the best order, and optical checking revealed a darkening of the irradiated area, indicating a decomposition of the sample (Figure 4). The black residue was most probably amorphous carbon due to decomposition. It is thus concluded that  $\text{SbC}_2\text{O}_4\text{OH}$  suffers radiation induced decomposition at  $\lambda = 112.684(1)$  pm, even for a beam of moderate intensity as present at beamline PDIFF of ANKA (Ångströmquelle Karlsruhe), whereas this effect does not occur at a laboratory X-ray diffractometer using  $\text{CuK}\alpha$  radiation.

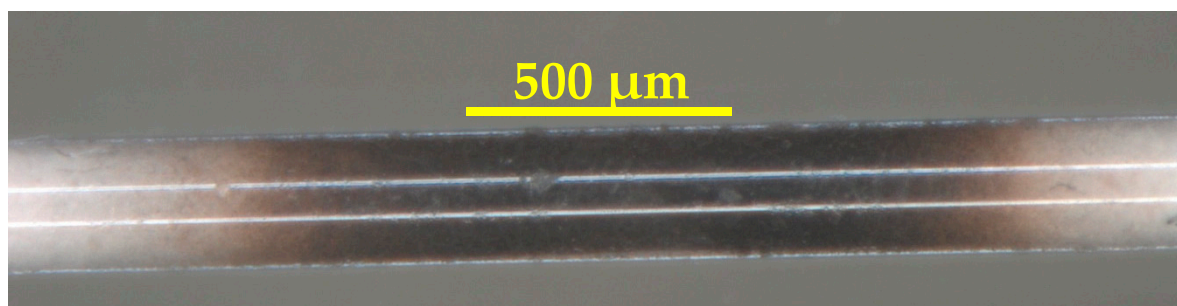


**Figure 4.** Glass capillary with 0.3 mm outer diameter filled with  $\text{SbC}_2\text{O}_4\text{OH}$  after exposure to synchrotron radiation ( $\lambda = 112.684(1)$  pm) for 1 h; the darkened area in the middle was exposed to the beam and probably contains amorphous carbon from the decomposition by radiation damage.



## 2.6. Chemical Reactions with $\text{SbC}_2\text{O}_4\text{OH}$ as a Precursor

$\text{SbC}_2\text{O}_4\text{OH}$  was reacted with Zn, ZnO or  $\text{ZnCO}_3$  in order to prepare ternary zinc antimony oxides. Heating a mixture of Zn with  $\text{SbC}_2\text{O}_4\text{OH}$  with a 10:1 molar ratio to 573 K under air overnight yielded ZnO as well as  $\text{Zn}_4\text{Sb}_3$  (Figure 5). Presumably, the carbon monoxide released during the decomposition of oxalate acts as a reducing agent for antimony. Further temperature treatment at 773 K yielded ZnO and  $\text{Sb}_2\text{O}_3$  by oxidizing the previously formed  $\text{Zn}_4\text{Sb}_3$ . Higher temperatures (973 K, Figure 5) lead to the formation of  $\text{ZnSb}_2\text{O}_6$ . Mixtures of ZnO with  $\text{SbC}_2\text{O}_4\text{OH}$  show decomposition of the latter to  $\text{Sb}_2\text{O}_3$  at 573 K. At higher temperatures (773 K and 973 K, Figure 6),  $\text{Sb}_2\text{O}_3$  is further oxidized to  $\text{Sb}_2\text{O}_4$ . ZnO does not participate in the reaction.  $\text{SbC}_2\text{O}_4\text{OH}$  reacts with  $\text{ZnCO}_3$  at 573 K to ZnO and  $\text{Sb}_2\text{O}_3$  (Figure 7). At higher temperatures (773 K and 973 K, Figure 7), ZnO and  $\text{Sb}_2\text{O}_3$  react to  $\text{ZnSb}_2\text{O}_6$ . Mixtures with higher content of  $\text{SbC}_2\text{O}_4\text{OH}$  (molar ratios of 4:3 and 1:2) behaved similarly.

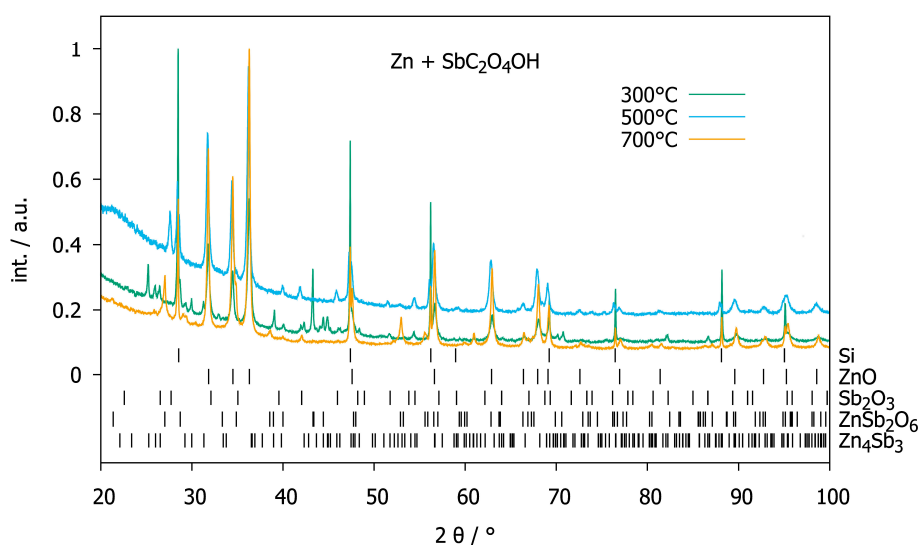


**Figure 5.** XRPD patterns (normalized intensities, Huber G670 diffractometer,  $\text{CuK}\alpha 1$  radiation, internal standard silicon powder) of a mixture of Zn and  $\text{SbC}_2\text{O}_4\text{OH}$  with a 10:1 molar ratio after heat treatment at 573 K (green), 773 K (blue) and 973 K (orange), respectively.

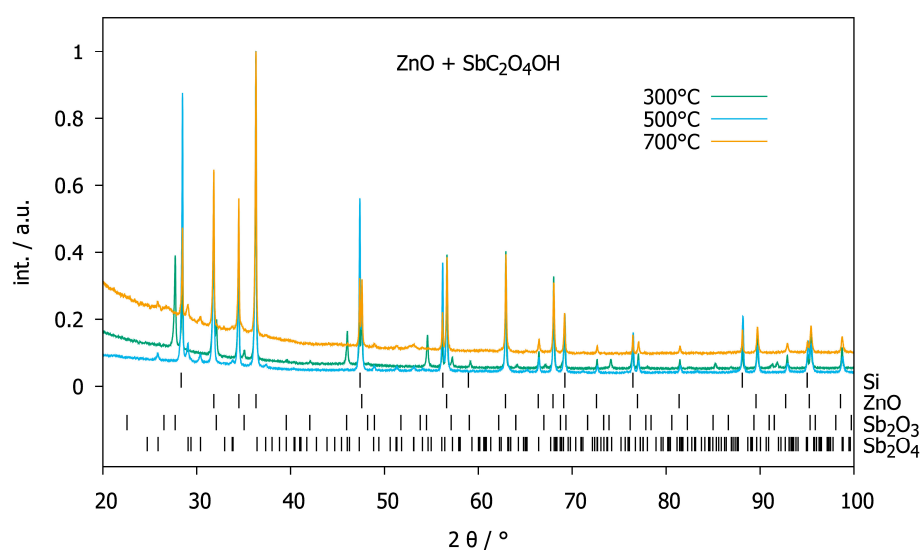


**Figure 6.** XRPD patterns (normalized intensities, Huber G670 diffractometer,  $\text{CuK}\alpha 1$  radiation, internal standard silicon powder) of a mixture of ZnO and  $\text{SbC}_2\text{O}_4\text{OH}$  with a 10:1 molar ratio after heat treatment at 573 K (green), 773 K (blue) and 973 K (orange), respectively.

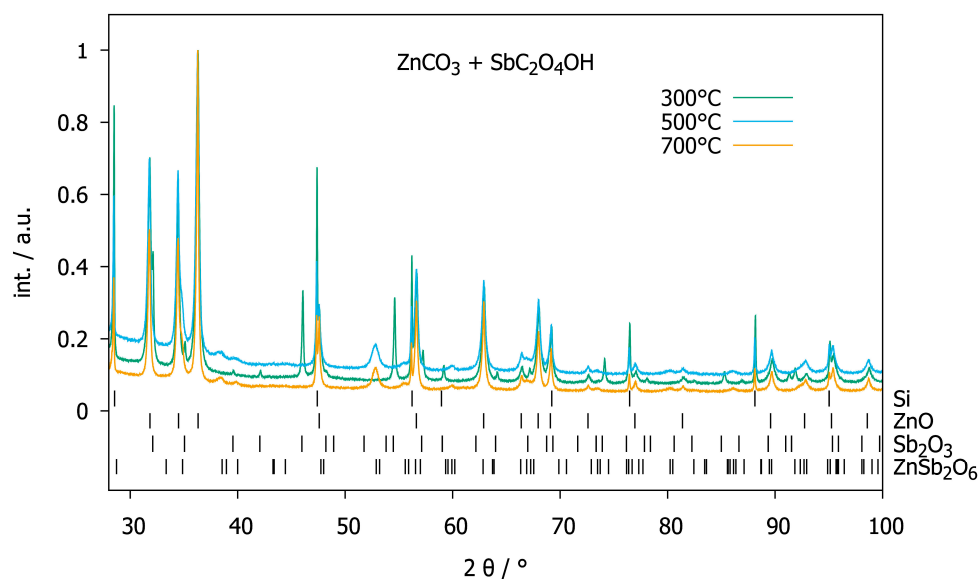


**Figure 7.** XRPD patterns (normalized intensities, Huber G670 diffractometer, CuK $\alpha$ 1 radiation, internal standard silicon powder) of a mixture of ZnCO<sub>3</sub> and SbC<sub>2</sub>O<sub>4</sub>OH with a 10:1 molar ratio after heat treatment at 573 K (green), 773 K (blue) and 973 K (orange), respectively.

### 3. Discussion

The deuteride SbC<sub>2</sub>O<sub>4</sub>OD can be synthesized by refluxing Sb<sub>2</sub>O<sub>3</sub> and water-free oxalic acid in D<sub>2</sub>O. It exhibits the same crystal structure as SbC<sub>2</sub>O<sub>4</sub>OH and shows the typical isotope effect, with a shift of the O–H stretching frequency by a factor of 1.35. Both SbC<sub>2</sub>O<sub>4</sub>OH and SbC<sub>2</sub>O<sub>4</sub>OD are rather inert considering H–D exchange. An SbC<sub>2</sub>O<sub>4</sub>OD sample may be stored in air for several months without any change in X-ray diffraction patterns and infrared spectra, with respect to one stored under argon. SbC<sub>2</sub>O<sub>4</sub>OH may even be refluxed in D<sub>2</sub>O without deuteration of the hydroxide group. In order to get an accurate picture of both the heavy and the light atoms in the crystal structure, the complementary methods of X-ray and neutron diffraction were used. The crystal structure exhibits zigzag chains of pentagonal SbO<sub>6</sub> pyramids linked by OH groups as primary units. They are linked by oxalate groups to build up a three-dimensional framework (Figure 8). Antimony ions show the one-sided coordination typical for *ns*<sup>2</sup> cations [13–15]. Sb–O, C–C and C–O interatomic distances are in the typical ranges for antimony oxides and oxalate ions, respectively. D–O distances are 97.6(10) pm within the OD group, and 204(1) pm to the neighboring oxalate ion, indicating the possibility of hydrogen bonds in the crystal structure. The crystal structure is in good agreement with the one found before by X-ray diffraction [10]. In SbC<sub>2</sub>O<sub>4</sub>OD deuterium atoms are disordered and located on either side of a mirror plane (*m* perpendicular to [010] in *Pnma*) with half occupation (Figure 8, Table 1). Quantum-mechanical studies showed that a fully ordered structure in space group *Pna*2<sub>1</sub> has a lower energy than the disordered one [10]. However, no signs for any ordering of deuterium atoms can be found by neutron diffraction. Disordered hydrogen atoms are not unusual, and order–disorder transitions occur in a wide range of hydrogenous materials [16–21].

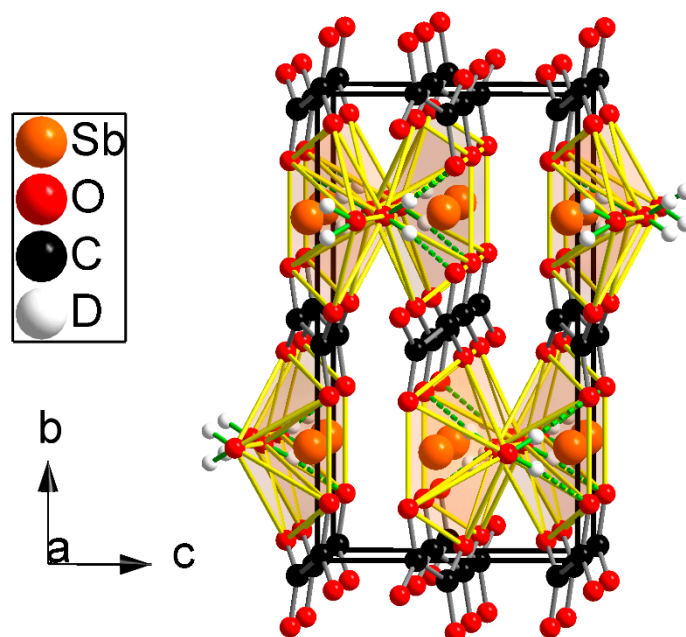


**Figure 8.** Crystal structure of  $\text{SbC}_2\text{O}_4\text{OD}$  as determined from neutron powder diffraction showing zigzag chains of pentagonal  $\text{SbO}_6$  pyramids along  $[100]$  linked by OD groups (split position for D atoms with half occupation) and oxalate anion bridging the chains. Selected interatomic distances are Sb–O1: 197.0(8) pm, Sb–O3:  $2 \times 224.6(6)$  pm, Sb–O2:  $2 \times 241.1(5)$  pm, Sb–O1: 244.7(8) pm, Sb–D:  $2 \times 247.7(10)$  pm, O1–D (green):  $2 \times 97.6(10)$  pm, O3–D (green dotted): 204(1) pm, C–O2: 125.8(5) pm, C–O3: 126.7(5), C–C: 151.5(5) pm.

$\text{SbC}_2\text{O}_4\text{OH}$  is not very stable with respect to heat and intense X-radiation. While the former gives antimony oxide, carbon dioxide, carbon monoxide and water at 564 K in an endothermic reaction, the latter leads to the formation of a dark amorphous residue, probably antimony oxide and carbon. The low decomposition temperature and easy handling of  $\text{SbC}_2\text{O}_4\text{OH}$  seem to be advantageous properties for a precursor in the synthesis of ternary oxides. This is put into perspective, however, by the results reaction of  $\text{SbC}_2\text{O}_4\text{OH}$  with reactants such as zinc, zinc oxide, and zinc carbonate. They react to ternary compounds like  $\text{ZnSb}_2\text{O}_6$ , at about the same temperatures as the mixtures of the binary oxides (1073 K [22]) do, way above the decomposition temperature of  $\text{SbC}_2\text{O}_4\text{OH}$ . Similar behavior was observed for the reaction of  $\text{SbC}_2\text{O}_4\text{OH}$ , with barium oxalate hydrate and bismuth oxide to  $\text{BaBi}_{1/2}\text{Sb}_{1/2}\text{O}_3$  [9]. The advantage of a low decomposition temperature is thus only an apparent one for the precursor-based synthesis of antimonates.

#### 4. Materials and Methods

**Synthesis:** 5.00 g  $\text{Sb}_2\text{O}_3$  (Riedel-de-Haën, Seelze, Germany, p.a.) and 4.40 g oxalic acid dehydrate (Riedel-de-Haën, Seelze, Germany, 98%) were refluxed in 60 mL deionized water for 3 h. The white residue of  $\text{SbC}_2\text{O}_4\text{OH}$  was filtered, washed with water, and dried at 388 K for 12 h. A deuterated sample  $\text{SbC}_2\text{O}_4\text{OD}$  was prepared in a similar way by using water-free oxalic acid and  $\text{D}_2\text{O}$ . Oxalic acid dihydrate (Riedel-de-Haën, Seelze, Germany, purum) was dried at 372 K for 2 h according to [23], ground, weighed and quickly transferred to a two-neck flask. There, 5.00 g  $\text{Sb}_2\text{O}_3$  (Riedel-de-Haën, Seelze, Germany, p.a.) and 3.14 g of the dried oxalic acid were refluxed in 60 mL  $\text{D}_2\text{O}$  (Eurisotop, Saint-Aubin, France, 99%) for 3 h. The white residue of  $\text{SbC}_2\text{O}_4\text{OD}$  was filtered, washed with  $\text{D}_2\text{O}$ , dried at 388 K for 12 h and kept in a desiccator. Reactions of  $\text{SbC}_2\text{O}_4\text{OH}$  with other metal precursors (Section 2.6) were carried out in open alumina crucibles at various temperatures. Mixtures of  $\text{SbC}_2\text{O}_4\text{OH}$  and Zn, ZnO, or  $\text{ZnCO}_3$  were intimately mixed and heated up to 1093 K for 12 h in order to investigate the behavior as a precursor for the synthesis of ternary zinc oxides. Resulting powders

were analyzed by X-ray powder diffraction. Refluxing of  $\text{SbC}_2\text{O}_4\text{OH}$  in  $\text{D}_2\text{O}$  did not give any H-D exchange, probably due to the low solubility of  $\text{SbC}_2\text{O}_4\text{OH}$ .

**Thermal analysis and emission gas analysis:** Thermal analysis was carried out on a 15.0 mg sample of  $\text{SbC}_2\text{O}_4\text{OH}$  in an alumina crucible in air on an STA409/414 (differential scanning calorimetry, DSC, and thermogravimetry, TG) (Netzsch, Selb, Germany) coupled by a skimmer to a quadrupole mass spectrometer QMG422 (Balzers, Hudson, NH, USA).

**Infrared spectroscopy:** Infrared spectra were recorded on a Tensor 27 FT-IR spectrometer (Bruker, Ettlingen, Germany) for  $400\text{ cm}^{-1} \leq \nu \leq 4000\text{ cm}^{-1}$  using KBr pellets.

**X-ray and synchrotron powder diffraction:** X-ray powder diffraction data were collected either using flat reflection samples containing an internal silicon standard on a diffractometer X'Pert (PANalytical, Almelo, The Netherlands) in Bragg-Brentano geometry at  $T = 296(1)\text{ K}$  with  $\text{CuK}\alpha$  radiation, or using flat transmission samples on a Huber G670 diffractometer in Guinier geometry and with  $\text{CuK}\alpha 1$  radiation. For the latter, samples were prepared by mixing the powders with an internal silicon standard and grease, and putting them between two sheets of capton foil. Rietveld refinements were carried out with the program FULLPROF [24–26] and pseudo-Voigt as the profile function. Synchrotron experiments were performed at the beamline PDIFF of ANKA (Ångströmquelle Karlsruhe) of the Karlsruher Institute of Technology (KIT) at a wavelength of  $\lambda = 112.684(1)\text{ pm}$ . The samples were contained in thin-walled glass capillaries with a 0.3 mm outer diameter.

**Neutron powder diffraction:** Neutron powder diffraction was carried out at the E9 diffractometer ( $\lambda = 1.79725\text{ \AA}$ ) at Helmholtz-Zentrum Berlin für Materialien und Energie, Berlin, Germany [27]. Powdered samples were held in thin-walled vanadium containers with a 6 mm inner diameter. Deuterides instead of hydrides were used in order to avoid the high incoherent scattering of  $^1\text{H}$  [12].

## 5. Conclusions

The synthesis of deuterated antimony oxalate hydroxide may be realized by slight modifications in the synthesis, i.e., use of water-free oxalic acid and  $\text{D}_2\text{O}$ . O–D stretching frequencies in  $\text{SbC}_2\text{O}_4\text{OD}$  are shifted by a factor of 1.35 with respect to O–H in  $\text{SbC}_2\text{O}_4\text{OH}$ . The crystal structure shows zigzag chains of pentagonal  $\text{SbO}_6$  pyramids linked by OH (OD) groups as the main structural features. Hydrogen (deuterium) atoms are disordered, i.e., occupy a position on either side of a mirror plane with half occupation and no preference for either one. Synchrotron radiation induces decomposition to an amorphous dark powder, probably antimony oxide and carbon.  $\text{SbC}_2\text{O}_4\text{OH}$  decomposes at low temperatures of 564 K to form  $\text{Sb}_2\text{O}_3$ ,  $\text{CO}_2$ , CO, and  $\text{H}_2\text{O}$ , which seems to be useful for synthesis of ternary oxides. This advantage is only an apparent one since the antimony oxide formed by the decomposition of  $\text{SbC}_2\text{O}_4\text{OH}$  reacts only at much higher temperatures to antimonates.

**Supplementary Materials:** The following are available online at <http://www.mdpi.com/2304-6740/8/3/21/s1>: CIF file and CheckCIF file for  $\text{SbC}_2\text{O}_4\text{OD}$ .

**Author Contributions:** Conceptualization, A.R., S.K. and H.K.; methodology, H.K. and A.R.; validation, A.R. and H.K.; formal analysis, A.R., S.K., and H.K.; investigation, A.R., S.K., H.K., and A.F.; resources, H.K.; data curation, H.K.; writing—original draft preparation, H.K.; writing—review and editing, A.R., S.K., H.K., A.F., and H.K.; visualization, A.R., S.K., H.K.; supervision, H.K.; project administration, H.K.; funding acquisition, H.K. All authors have read and agreed to the published version of the manuscript.

**Funding:** This research received no external funding.

**Acknowledgments:** We thank Johannes Moldrickx (Leipzig University) for help with H/D exchange studies in  $\text{SbC}_2\text{O}_4\text{OH}$  and Sara Schmorl (Leipzig University) for measuring IR spectra.

**Conflicts of Interest:** The authors declare no conflict of interest. The company (CM CHEMIEMETALL GmbH) had no role in the design of the study; in the collection, analyses, or interpretation of data; in the writing of the manuscript, or in the decision to publish the results.

## References

1. Lu, J.; Li, Y.; Zhao, K.; Xu, J.Q.; Ju, J.H.; Li, G.H.; Zhang, X.; Bie, H.Y.; Wang, T.G. Novel oxalate coordination mode and roles: Synthesis, structure and fluorescence property of  $[\text{Cd}_2(\mu\text{-ox})(\mu_3\text{-OH})_2]$  with 3-D structure. *Inorg. Chem. Commun.* **2004**, *7*, 1154–1156. [[CrossRef](#)]
2. Hamdouni, M.; Walha, S.; Kabadou, A.; Duhayon, C.; Sutter, J.P. Synthesis and crystal structures of various phases of the microporous three-dimensional coordination polymer  $[\text{Zr}(\text{OH})_2(\text{C}_2\text{O}_4)]$ . *Cryst. Growth Des.* **2013**, *13*, 5100–5106. [[CrossRef](#)]
3. Rivenet, M.; Roussel, P.; Abraham, F. One-dimensional inorganic arrangement in the bismuth oxalate hydroxide  $\text{Bi}(\text{C}_2\text{O}_4)\text{OH}$ . *J. Solid State Chem.* **2008**, *181*, 2586–2590. [[CrossRef](#)]
4. Roumanille, P.; Baco-Carles, V.; Bonningue, C.; Gougeon, M.; Duployer, B.; Monfraix, P.; Trong, H.L.; Tailhades, P.  $\text{Bi}_2(\text{C}_2\text{O}_4)_3 \cdot 7\text{H}_2\text{O}$  and  $\text{Bi}(\text{C}_2\text{O}_4)\text{OH}$  Oxalates Thermal Decomposition Revisited. Formation of Nanoparticles with a Lower Melting Point than Bulk Bismuth. *Inorg. Chem.* **2017**, *56*, 9486–9496. [[CrossRef](#)]
5. Nanda, B.N.; Pani, S. Diaquo-mono-oxalato-antimony complex. *J. Ind. Chem. Soc.* **1957**, *34*, 481–485.
6. Ambe, S. Chemical properties of  $\text{Sb}(\text{III})(\text{C}_2\text{O}_4)\text{OH}$ . *J. Inorg. Nucl. Chem.* **1975**, *37*, 2023. [[CrossRef](#)]
7. Ambe, S.; Ambe, F. Mössbauer emission spectrum of  $^{119}\text{Sn}$  in  $^{119}\text{Sb}(\text{OH})(\text{C}_2\text{O}_4)$ . *Inorg. Nucl. Chem. Lett.* **1975**, *11*, 139–143. [[CrossRef](#)]
8. Karlov, V.P.; Btutzov, G.N.; Dobrokhotova, T.F. Preparation and Properties of Antimony(III) Oxalate. *Russ. J. Inorg. Chem. (Transl. Zh. Neorg. Khim.)* **1983**, *28*, 1218–1219.
9. Korzun, B.V.; Schorr, S.; Schmitz, W.; Fadzeyeva, A.A.; Kommichau, G.; Bente, K. Preparation of  $\text{BaBi}_{1/2}\text{Sb}_{1/2}\text{O}_3$  from  $\text{Ba}(\text{COO})_2 \cdot 0.5\text{H}_2\text{O}$  and  $\text{Sb}(\text{COO})_2(\text{OH})$  oxalates and  $\text{Bi}_2\text{O}_3$  oxide. *J. Cryst. Growth* **2005**, *277*, 205–209. [[CrossRef](#)]
10. Kaduk, J.A.; Toft, M.A.; Golab, J.T. Crystal structure of antimony oxalate hydroxide,  $\text{Sb}(\text{C}_2\text{O}_4)\text{OH}$ . *Powder Diffr.* **2010**, *25*, 19–24. [[CrossRef](#)]
11. de Oliveira, E.F.; Hase, Y. Infrared study and isotopic effect of magnesium hydroxide. *Vib. Spectrosc.* **2001**, *25*, 53–56. [[CrossRef](#)]
12. Sears, V.F. Neutron scattering lengths and cross sections. *Neutron News* **1992**, *3*, 26–37. [[CrossRef](#)]
13. Halasyamani, P.S. Asymmetric Cation Coordination in Oxide Materials: Influence of Lone-Pair Cations on the Intra-octahedral Distortion in  $d^0$  Transition Metals. *Chem. Mater.* **2004**, *16*, 3586–3592. [[CrossRef](#)]
14. Beck, H.P.; Tratzky, H.; Kallmayer, V.; Stöwe, K. The  $\text{InSnCl}_3$ -Type Arrangement. I. A New  $\text{ABX}_3$  Structure Type with Close Cation-Cation Contacts. *J. Solid State Chem.* **1999**, *146*, 344–350. [[CrossRef](#)]
15. Walsh, A.; Payne, D.J.; Egddell, R.G.; Watson, G.W. Stereochemistry of post-transition metal oxides: Revision of the classical lone pair model. *Chem. Soc. Rev.* **2011**, *40*, 4455–4463. [[CrossRef](#)] [[PubMed](#)]
16. Hill, R.J. Hydrogen and order—Disorder in  $\text{PbO}_2$  in lead/acid positive plates. *J. Power Sources* **1989**, *25*, 313–320. [[CrossRef](#)]
17. Tabatabaee, M.; Poupon, M.; Eigner, V.; Vanek, P.; Dusek, M. The role of hydrogen bonds in order-disorder transition of a new incommensurate low temperature phase  $\beta\text{-}[\text{Zn}(\text{C}_7\text{H}_4\text{NO}_4)_2] \cdot 3\text{H}_2\text{O}$ . *Z. Kristallogr.* **2018**, *233*, 17–25. [[CrossRef](#)]
18. Kohlmann, H.; Moyer, R.O., Jr.; Hansen, T.; Yvon, K. X-ray and neutron powder diffraction study of the order-disorder transition in  $\text{Eu}_2\text{IrH}_5$  and the mixed crystal compounds  $\text{Eu}_{2-x}\text{A}_x\text{IrH}_5$  ( $\text{A} = \text{Ca}, \text{Sr}; x = 1.0, 1.5$ ). *J. Solid State Chem.* **2003**, *174*, 35–43. [[CrossRef](#)]
19. Kohlmann, H.; Yvon, K. Revision of the low-temperature structures of rhombohedral  $\text{ZrCr}_2\text{D}_x$  ( $x \sim 3.8$ ), and monoclinic  $\text{ZrV}_2\text{D}_x$  ( $1.1 < x < 2.3$ ) and  $\text{HfV}_2\text{D}_x$  ( $x \sim 1.9$ ). *J. Alloys Compd.* **2000**, *309*, 123–126.
20. Kohlmann, H.; Fauth, F.; Fischer, P.; Skripov, A.V.; Yvon, K. Low-temperature deuterium ordering in the cubic Laves phase derivative  $\alpha\text{-ZrCr}_2\text{D}_{0.66}$ . *J. Alloys Compd.* **2001**, *327*, L4–L9. [[CrossRef](#)]
21. Petrov, I.; Petrushevski, V.; Al-kassab, A.W.; Liesegang, J.; James, B.D. Effect of Deuteration on Order-Disorder in Hydrogen Disulfate Compounds,  $\text{M}_3\text{H}(\text{SO}_4)_2$  ( $\text{M} = \text{Na}, \text{K}, \text{Rb}, \text{Cs}, \text{NH}_4$ ). *Spectr. Lett.* **1988**, *21*, 167–182. [[CrossRef](#)]
22. Kumari, K.G.V.; Vasu, P.D.; Kumar, V.; Aoslán, T. Formation of Zinc–Antimony-Based Spinel Phases. *J. Am. Ceram. Soc.* **2002**, *85*, 703–705. [[CrossRef](#)]
23. Bowden, E. Oxalic acid (Anhydrous). *Org. Synth.* **1921**, *1*, 67.
24. Rodriguez-Carvajal, J. Recent advances in magnetic structure determination neutron powder diffraction. *Z. Phys. B Condens. Matter* **1993**, *192*, 55–69. [[CrossRef](#)]



25. FULLPROF, version 5; Rodriguez-Carvajal, J. (ILL): Grenoble, France, 2012.
26. Rodriguez-Carvajal, J. Recent Developments of the Program FULLPROF. *Comm. Powder Diffr. (IUCr) Newsl.* **2001**, *26*, 12–19.
27. Franz, A.; Hoser, A. E9: The Fine Resolution Powder Diffractometer (FIREPOD) at BER II. *J. Large Scale Res. Facil.* **2017**, *3*, A103. [[CrossRef](#)]



© 2020 by the authors. Licensee MDPI, Basel, Switzerland. This article is an open access article distributed under the terms and conditions of the Creative Commons Attribution (CC BY) license (<http://creativecommons.org/licenses/by/4.0/>).